Pressure peaking phenomenon for indoor hydrogen releases

Elsevier Editorial System(tm) for
International Journal of Hydrogen Energy
Manuscript Draft

Manuscript Number: HE-D-18-01942R1

Title: Pressure peaking phenomenon for indoor hydrogen releases

Article Type: Full Length Article

Section/Category: Safety / Sensors

Keywords: Pressure peaking; hydrogen; enclosure; ventilation; overpressure; nomogram

Corresponding Author: Dr. Sile Louise Brennan, Ph.D

Corresponding Author's Institution: Ulster University

First Author: Sile Louise Brennan, Ph.D

Order of Authors: Sile Louise Brennan, Ph.D

Abstract: The pressure peaking phenomenon can be observed when hydrogen is released in enclosures with vent(s). The unforeseen physical phenomena of pressure peaking has been described and explained. This phenomenon occurs for hydrogen releases in enclosures where the vent(s), volume, and leak rate are such that there will be no air ingress to the enclosure. Pressure peaking describes the physical phenomenon of a peak in the pressure transient during such a release for some release conditions in a vented enclosure. This phenomenon is pronounced only for gases lighter than air, e.g. hydrogen and helium. For particular release flow rates and vent sizes the peak can be an order of magnitude higher compared to the steady-state overpressure that is reached when the enclosure is fully filled with hydrogen over time. This finding is relevant to all hydrogen applications indoors from a fuel cell in an enclosure or laboratory scale storage up to a forklift in a warehouse. The peak magnitude depends on the release flow rate, hydrogen inventory, enclosure volume and the ventilation area, and potentially can exceed the maximum pressure which the enclosure can withstand. A look up nomogram for applicability of the developed theory that is based on vent area and leak rate has been created for sustained releases. Experimental evidence of the phenomena is described. Reduced analytical equations are presented for the case of a constant flow rate release, and the associated nomogram is presented for use by hydrogen safety engineers and regulators.

Highlights

- Describes and explains the pressure peaking phenomena for indoor hydrogen releases
- Occurs when leak and geometry configuration lead to no air ingress to the enclosure
- Nomogram to calculate peak overpressure for constant leak rate in an enclosure
- Reduced analytical equations are given
- Tools presented for use by hydrogen safety engineers and regulators

Pressure peaking phenomenon for indoor hydrogen releases

Sile Brennan* and Vladimir Molkov
*Corresponding author email: sl.brennan@ulster.ac.uk
Hydrogen Safety Engineering and Research Centre (HySAFER), University of Ulster, Newtownabbey BT37 0QB, UK

Abstract

The pressure peaking phenomenon can be observed when hydrogen is released in enclosures with vent(s). The unforeseen physical phenomena of pressure peaking has been described and explained. This phenomenon occurs for hydrogen releases in enclosures where the vent(s), volume, and leak rate are such that there will be no air ingress to the enclosure. Pressure peaking describes the physical phenomenon of a peak in the pressure transient during such a release for some release conditions in a vented enclosure. This phenomenon is pronounced only for gases lighter than air, e.g. hydrogen and helium. For particular release flow rates and vent sizes the peak can be an order of magnitude higher compared to the steady-state overpressure that is reached when the enclosure is fully filled with hydrogen over time. This finding is relevant to all hydrogen applications indoors from a fuel cell in an enclosure or laboratory scale storage up to a forklift in a warehouse. The peak magnitude depends on the release flow rate, hydrogen inventory, enclosure volume and the ventilation area, and potentially can exceed the maximum pressure which the enclosure can withstand. A look up nomogram for applicability of the developed theory that is based on vent area and leak rate has been created for sustained releases. Experimental evidence of the phenomena is described. Reduced analytical equations are presented for the case of a constant flow rate release, and the associated nomogram is presented for use by hydrogen safety engineers and regulators.

Keywords

Pressure peaking, hydrogen, enclosure, ventilation, overpressure, nomogram

Nomenclature

General		**Greek**	
A	vent area (m^2)	γ	ratio of specific heats
C	coefficient of discharge	ρ	density (kg/m^3)
h	vent height (m)	**Subscripts and superscripts**	
M	molecular mass (kg/mol)	$_a$	Air
$\dot{m}$	mass flow rate (kg/s)	$_{atm}$	Atmospheric
m	mass (kg)	$_{encl}$	enclosure
n	number of moles	$_h$	Hydrogen
P	pressure (Pa)	$_{nozz}$	Nozzle
R	universal gas constant	$_t$	Time
T	temperature	$_{max}$	Maximum
V	volume (m^3)	$_{vent}$	Vent
$\dot{V}$	volumetric flow rate (m^3/s)	**Acronyms**	
v	velocity (m/s)	CFD	Computational Fluid Dynamics
X	mole fraction	PRD	Pressure Relief Device
Y	mass fraction		

1.0 Introduction

As hydrogen and fuel cell applications become more widely used it is practical that their indoor use is considered and understood. Necessary indoor use of these systems is unavoidable, and examples include fuel cells or hydrogen storage in a confined space or enclosures, hydrogen vehicles in garages or maintenance shops, hydrogen powered forklifts in warehouses, production and storage in research laboratories, there are numerous applications. There is a clear need to understand the hazards associated with indoor use in order to provide

guidance, inform standards, and ensure inherently safer design. The work presented here is motivated by the need to better understand the safety issues surrounding indoor use of hydrogen and fuel cell applications to inform engineers so that the effects of potential hazards may be mitigated against or prevented through design. The topic is timely and hence is the subject of on-going investigations by a number of research groups globally as evidenced by recent publications for example [1] and [2], it has been the subject of European research project HyIndoor [**Error! Reference source not found.**].

From a safety perspective, a number of hazards arise following an unignited hydrogen release in a vented enclosure. Previous works e.g. [4, 5] have focused on dispersion, and formation of a flammable atmosphere in an enclosure for comparatively small releases. Whilst the dynamics of hydrogen concentration are briefly discussed here, this work focuses primarily on overpressure development and tools that can be used to predict, and thus potentially avoid, excessive overpressure capable of demolishing a structure for releases indoors.

Previous work by the authors [6, 7] has introduced the phenomena of pressure peaking during a non-reacting release from hydrogen storage through a pressure relief device (PRD) in an enclosure with a vent. The initial study was driven by the need to understand the potential safety issues associated with parking a vehicle in a garage with the aim of informing guidance, however the findings are applicable to any application where the vent(s), volume, and leak rate are such that there will be no air ingress to the enclosure. The initial work [6] described the case of a sustained release with a constant mass flow rate from 3 MPa storage through a 5.08 mm diameter PRD in a garage-like enclosure of volume 30.4 m^3 with a single brick-like vent of size 250x50 mm. Computational Fluid Dynamics (CFD) was used to demonstrate the occurrence of a peak in the pressure dynamics (pressure-time curve) following the injection of hydrogen in the enclosure. A system of equations was presented describing this phenomenon. It was demonstrated how the overpressure levels in the case chosen were capable of causing major damage and possible collapse within only 1 s even without ignition. This phenomenon was shown to be pronounced only for hydrogen and to some small extent for methane but not for other combustible gases with a molecular mass higher than air. It was shown in [6] that if the enclosure does not rupture first (i.e. collapse), the pressure within the garage, reaches a maximum level in excess of 60 kPa for 35 MPa storage. This maximum pressure then drops off and tends towards a steady state value, an order of magnitude lower, and equal to that predicted by the simple steady state estimations of pure hydrogen release from the enclosure i.e. 17 kPa [6].

Subsequent work [7] accounted for a decrease in tank pressure during hydrogen blow down and hence a decreasing mass flow rate. A blow down model developed at the University of Ulster and published elsewhere [9, 10] was used to determine mass flow rate from a hydrogen storage tank and this mass flow rate was used as an input to the pressure peaking model. An attempt was made in [7] to correlate Air Change per Hour (ACH) with vent size and enclosure volume and use this to develop a nomogram for "safe" PRD diameters. In [7] a "safe" diameter was defined as that which, for a given enclosure volume and vent size, would result in a "pressure peak" or overpressure which was considered to be "safe" for the structure. Overpressure levels not exceeding 20 kPa where deemed to be sufficiently low to avoid serious structural failure. The "safe" diameters indicated in [7] are significantly smaller than those typically used in existing PRDs. However, as a PRD diameter is decreased the hydrogen will naturally take a longer time to blow down from the storage tank. Hence it is clear that the fire resistance of the tanks has to be increased in-line with the blow down time to avoid both catastrophic tank failure in fire, and destruction of the enclosure by the pressure peaking phenomenon. The nomograms presented in [7] give a "safe" diameter and subsequent blow down time for a specific enclosure volume, ACH, and hydrogen storage pressure and inventory. Whilst the authors do believe that the nomograms presented in [7] could be used as an engineering tool, neither the diameters nor the blow down times suggested may be feasible in practice for today's storage tanks, with their current level of fire resistance. The work in [7]

rather serves to highlight the existing problem for the benefit of future tank design with increased fire resistance.

Both previous works [6, 7] focused on the case of a malfunctioning PRD and hence a relatively high mass flow rate in an enclosure. In the case of [7] it is also noted that there is ambiguity in the literature regarding the method used to calculate ACH. The authors believe that the pressure peaking phenomenon is widely applicable and should be accounted for in design for all indoor hydrogen and fuel cell applications ranging from small fuel cell enclosures and laboratory applications to maintenance shops etc. Indeed, recent work [8] has validated the phenomenon in a laboratory scale enclosure typical with dimensions and leak rates characteristic of a fuel cell. This work seeks to clarify the phenomena for an unignited release, present usable hydrogen safety engineering tools to inform design and the permitting processes and highlights the need to perform analysis for an ignited case, a scenario also under consideration by the authors [16].

2.0 Problem description

As previously mentioned, indoor use of hydrogen and fuel cell systems covers a wide range of potential scenarios; a fuel cell in a 1 m^3 cabinet and a forklift in a 1000 m^3 warehouse are just two of many possible cases. The potential leak rates encountered may range from fractions of a gram per second (g/s) for partial ruptures of low pressure pipes, close to 0.5 kg/s when considering a constant release following full bore rupture of a PRD with a diameter about 5 mm on a 70 MPa storage tank, or indeed larger rates if releases from higher pressures or pipe diameters are taken into account.

In this work a range of scenarios are examined whereby a hydrogen release occurs in a vented enclosure. Releases from hydrogen storage at pressure of 1–100 MPa through leak diameters ranging from 0.1–25 mm are considered. These pressure and diameter ranges were deemed to be representative of values encountered in existing applications. Although it is the belief of the authors that some of the configurations met in practice are not always deemed to be within acceptable safety reasoning.

One purpose of the work presented here is to develop a usable nomogram for hydrogen safety engineers and regulators relating storage pressure, leak diameter and enclosure vent size to the resultant pressure peak. In developing the nomogram it should be emphasised that a constant mass flow rate (sustained) release is taken as a conservative case, rather than accounting for blow-down. However, it should also be noted that for the high-pressure releases, pressure peaking occurs within a matter of seconds, before the point at which the leak rate has reduced significantly. For a constant release rate overpressures were calculated for a range of pressure, diameter, and vent area scenarios. In order to limit the quantity of data and present it in a usable and applicable format only scenarios leading to overpressures in the region of 1–100 kPa are included in the nomogram. Hess et al. [11] present values of 15-20 kPa as capable of causing collapse of unreinforced concrete or cinderblock walls, and 20-30 kPa as capable of causing collapse of industrial steel frame structure and 1-10 kPa peak overpressure is needed to break glass windows [12]. Hence a range of 0-100 kPa in this study was deemed to cover the range of overpressures likely to be considered by an end user.

3.0 Methodology

A phenomenological model of the pressure peaking phenomenon [6] has been used to estimate overpressure in a vented enclosure, this model predicts the transient pressure in the enclosure. In order to calculate the mass flow rate from storage with a given pressure through a given orifice diameter the under-expanded jet theory for a non-ideal gas was applied [9, 10].

In the cases presented, where blow down is considered, the output (mass flow rate) of the isothermal model [10] is used as an input to the phenomenological model of the pressure peaking phenomenon. This model takes into account the under-expanded jet theory [9] and

can be used to calculate decay of pressure and transient mass flow rate during a release from a storage tank of known volume through an orifice of known diameter.

3.1 Model description

Former simple models applied to estimate the steady state overpressure within an enclosure were shown in [6] to considerably under-predict the maximum overpressure in an enclosure as they do not account for the recently revealed dynamic phenomenon of pressure peaking. Instead a system of equations shown below [6] is used to predict the development of the overpressure within the enclosure with time in the assumption of a perfect mixing of each released fraction of hydrogen with the mixture already available within the garage i.e. uniform concentration,

$$m_{encl}^{t+\Delta t} = m_{encl}^{t} + (\dot{m}_{nozz}^{t} - \dot{m}_{vent}^{t})\Delta t \tag{1}$$

$$n_{encl}^{t+\Delta t} = n_{encl}^{t} + \left(\frac{\dot{m}_{nozz}^{t}}{M_{H_2}} - \frac{\dot{m}_{vent}^{t} n_{encl}^{t}}{m_{encl}^{t}}\right)\Delta t \tag{2}$$

$$P_{encl(t_{a+1})} = \frac{n_{encl}^{t+\Delta t} RT}{V}, \tag{3}$$

$$\dot{m}_{vent}^{t+\Delta t} = C\left(\frac{m_{encl}^{t+\Delta t} A}{V}\right)\left(\frac{2\left(P_{encl}^{t+\Delta t} - P_0\right)V}{m_{encl}^{t+\Delta t}}\right)^{\frac{1}{2}}. \tag{4}$$

In this system of equations m is the mass, M is the molecular mass, n is the number of moles, R is the universal gas constant, T is the temperature, t is time, V is the volume, and C is the discharge coefficient which is taken here as 0.6 based on both a comparison with CFD simulations [6] and data from the literature [13].

As mentioned the phenomenological model assumes a perfectly stirred reactor hence gradients of concentration and pressure within the vessel are not accounted for. The model is applicable for releases where the flow is out of the enclosure through the whole area of the vent(s) and there is no air ingress, i.e. releases that would lead to 100% of hydrogen accumulation in a vented enclosure with time [1]. The model does not account for vent location or shape and is based purely on total vent area, nor does it account for leak location or direction (well-mixed regime of release). Simulation work, with varying vent size and orientation has been performed to assess the limits of this assumption, and the authors have found the phenomenological model to predict maximum pressure and dynamics reasonably well in all cases where there is no air ingress. In a limited number of cases, where vent orientation results in a period of time with only air exiting the vent there is a negligible dip in the pressure dynamics curve for the simulation compared to the phenomenological model however, the difference in pressure is of the order of <5%.

3.2 Examples and explanation of the pressure-peaking phenomena

Figure 1 illustrates the pressure dynamics for a constant mass flow rate release of 1 g/s (characteristic of that used to feed a 50 kW fuel cell) in a 1 m^3 enclosure with a vent of 1x1 cm. Figure 2 shows the pressure dynamics for a constant mass flow rate release of 390 g/s (characteristic of a release from 35 MPa storage through a 5.08 mm diameter PRD orifice) in a 30 m^3 enclosure with a vent of 20x20 cm.

Figure 1. Overpressure versus time for a constant mass flow rate release of 1 g/s in a 1 m^3 enclosure with a 1 cm by 1 cm vent.

Figure 2. Overpressure versus time for a constant mass flow rate release of 390 g/s in a 30 m^3 enclosure with a 20 cm by 20 cm vent.

From Figs. 1 and 2 it can be seen that there is a peak in overpressure with time rather than monotonic increase of pressure to the steady-state value. This phenomenon is described as pressure peaking. As mentioned, this phenomenon is pronounced only for gases lighter than air and stems from the difference in the molecular mass of hydrogen and air. Therefore, the lower molecular mass, the more pronounced the effect. Thus, whilst not a combustible gas, the behaviour can also be seen with helium. Figure 3 illustrates the overpressure in a 30.4 m^3 enclosure (typical garage) with a single vent of 250x50 mm for releases of hydrogen, helium, methane and propane from a 35 MPa storage through a 5.08 mm diameter orifice PRD. The release rate is assumed constant and was calculated for each gas respectively (H_2 = 390 g/s, He_2 = 490 g/s, CH_4 = 609 g/s and C_3H_8 = 568 g/s (this scenario is hypothetical for propane as it cannot be stored at such high pressure at normal conditions). It is clear from Fig. 3 that hydrogen is the only combustible gas for which the phenomenon is significant and has potential safety implications. It is seen that while methane has a hardly distinguishable peak, propane has no peak at all.

Figure 3. Overpressure versus time for a constant mass flow rate releases of hydrogen, helium, methane and propane from a 5.08 mm diameter PRD from 35 MPa storage in a 30.4 m^3 enclosure with a 250 mm x 50 mm vent.

In order to understand the pressure peaking phenomenon, consider Equation 3 (the ideal gas law) which describes the pressure at a given point in time. From this equation it is clear that pressure is at a maximum when the number of moles in the enclosure is at a maximum. Equation 2 describes the number of moles in the enclosure at a given point in time and can be rewritten as

$$n_{encl}^{t+\Delta t} = n_{encl}^{t} + \left(\frac{\dot{m}_{nozz}^{t}}{M_h} - \frac{\dot{m}_{vent}^{t}}{M_{encl}}\right)\Delta t \tag{5}$$

where M_{encl} represents the average molecular mass of the mixture in the enclosure which will be equal to the molecular mass of air at *t=0* and will decrease with time until the enclosure is completely filled with hydrogen. Initially, at *t=0* there will be no flow out of the vent. Considering a constant leak rate, when a steady state is reached the mass flow into the enclosure will equal the mass flow rate out. As the release progresses, the rate of moles entering the enclosure is a constant i.e. $\frac{\dot{m}_{nozz}^{t}}{M_h}$ is a constant. For a fixed mass flow rate release it is clear that the molar flow rate is considerably higher for hydrogen than other fuels given hydrogen's low molecular mass M_h. Thus from Equation 5 it can be seen that when $\frac{\dot{m}_{nozz}^{t}}{M_h}$ is a constant then the number of moles in the enclosure, and hence pressure will either be decreasing or increasing depending on if $\frac{\dot{m}_{vent}^{t}}{M_{encl}}$is greater or less than $\frac{\dot{m}_{nozz}^{t}}{M_h}$. Equation 4 describes the mass flow rate at the vent and can be rewritten in terms of density in the enclosure ρ_{encl} as:

$$\dot{m}_{vent}^{t+\Delta t} = C\rho_{encl}^{t+\Delta t} A \left(\frac{2\left(P_{encl}^{t+\Delta t} - P_0\right)}{\rho_{encl}^{t+\Delta t}}\right)^{\frac{1}{2}}. \tag{6}$$

It can also be useful to think of the problem in terms of volumetric flow rates $\dot{V}$, and the volumetric flow rate through the vent can be written as,

$$\dot{V}_{vent}^{t+\Delta t} = CA\left(\frac{2\left(P_{encl}^{t+\Delta t} - P_0\right)}{\rho_{encl}^{t+\Delta t}}\right)^{\frac{1}{2}}. \quad (7)$$

In the case of a sustained release with constant flow rate then both the mass flow rate and the volumetric flow rate into the enclosure will not change with time, whereas the mass flow rate and volumetric flow rate out of the enclosure, as described by equation 6 and 7 respectively will change.

It is clear from equation 7, that volumetric flow rate through the vent is proportional to $\sqrt{\Delta P_{encl}}$ and inversely proportional to $\sqrt{\rho_{encl}}$. Density in the enclosure ρ_{encl} is a maximum at time zero when it is equal to that of air and is a minimum when the enclosure is filled with hydrogen, similarly the average molecular mass in the enclosure M_{encl} is a maximum at time zero when it is equal to that of air i.e. both ρ_{encl} and M_{encl} approach minimum values of ρ_h and M_h respectively. In the beginning of the process when the density of the enclosure mixture ρ_{encl} is comparatively high, and close to that of air then the constant volumetric flow rate of hydrogen into the enclosure is above the volumetric outflow of heavier hydrogen-air mixture out of the enclosure. The pressure within the enclosure grows to allow the mass flow rate of the outgoing gas (function of pressure Eq. 6) to match the constant (for this scenario) mass flow rate entering the enclosure from the leak. Then, the molecular mass of hydrogen-air mixture decreases with time as there is no air entering the enclosure due to the high release rate of the leak (condition of model). This implies that the volumetric flow rate increases, thus the pressure in the enclosure can drop to match the constant volumetric flow rate from the leak.

The enclosure pressure dynamics may also be understood in terms of moles. The pressure in the enclosure ΔP_{encl} depends on the number of moles in the enclosure (Equation 3). ΔP_{encl} will increase so long as the rate of moles entering the enclosure is greater than the rate of moles out through the vent i.e. $\frac{\dot{m}_{vent}^t}{M_{encl}} < \frac{\dot{m}_{nozz}^t}{M_h}$ (from Equation 5). ΔP_{encl} will decrease when $\frac{\dot{m}_{vent}^t}{M_{encl}} > \frac{\dot{m}_{nozz}^t}{M_h}$ and thus ΔP_{encl} will be at a maximum when $\frac{\dot{m}_{vent}^t}{M_{encl}} = \frac{\dot{m}_{nozz}^t}{M_h}$. The term $\frac{\dot{m}_{nozz}^t}{M_h}$ is a constant when the release rate is sustained at a constant flow rate, so in order to understand how pressure behaves in the enclosure for the case of a constant release rate then the term $\frac{\dot{m}_{vent}^t}{M_{encl}}$ should be considered; as mentioned M_{encl} will be at a maximum at the start of the release and will monotonically decrease in value, the behaviour of $\dot{m}_{vent}$ is more complex.

At the start of the release ρ_{encl} is at a maximum, the volumetric and mass flow rates out of the enclosure are therefore less than the flow rates in to the enclosure as described above i.e. $\dot{V}_{vent} < \dot{V}_{nozz}$ and $\dot{m}_{vent} < \dot{m}_{nozz}$. Initially $\frac{\dot{m}_{vent}^t}{M_{encl}}$ will be at a minimum, thus the number of moles in the enclosure will grow and hence ΔP_{encl} will increase. However, as ΔP_{encl} increases, $\dot{V}_{vent}$ increases according to Equation 7 and $\dot{m}_{vent}$ increases according to Equation 6, while ρ_{encl} continuously decreases. As long as $\frac{\dot{m}_{vent}^t}{M_{encl}} < \frac{\dot{m}_{nozz}^t}{M_h}$ then ΔP_{encl} will increase and thus $\dot{V}_{vent}$ and $\dot{m}_{vent}$ will continue to increase. A situation will be reached whereby $\frac{\dot{m}_{vent}^t}{M_{encl}} = \frac{\dot{m}_{nozz}^t}{M_h}$. At this point the number of moles entering the enclosure is equal to the number of moles exiting the enclosure and pressure is at a maximum possible value (gradient of pressure in time is zero), pressure can no longer continue to grow, as the release continues

ρ_{encl} will decrease. If ΔP_{encl} is not growing with time and ρ_{encl} is decreasing then $\dot{m}_{vent}$ decreases as per Equation 6 and $\dot{V}_{vent}$ also decreases. As $\dot{m}_{vent}$ is decreasing, M_{encl} is also decreasing and the term $\frac{\dot{m}^t_{vent}}{M_{encl}}$ converges towards $\frac{\dot{m}^t_{nozz}}{M_h}$, i.e. steady state where gradient of pressure in time is zero. Eventually, ΔP_{encl} , $\dot{V}_{vent}$ and $\dot{m}_{vent}$ will reach a steady state value.

Hence, for the case of a constant leak rate $\dot{m}_{nozz}$ in an enclosure with a vent the volumetric flow rate out of the enclosure vent(s) $\dot{V}_{vent}$, the enclosure overpressure ΔP_{encl} and the mass flow rate out of the vent $\dot{m}_{vent}$ will all exhibit peaking behaviour if a gas which is lighter than air is released into the vented enclosure.

The dynamics of mass flow rate and volumetric flow rate at the vent, and overpressure in the enclosure for a constant mass flow rate release of 390 g/s in a 30 m^3 enclosure with a 20 cm by 20 cm vent are shown in Fig. 4. All exhibit a peak.

Figure 4. Overpressure in the enclosure, volumetric and mass flow rate at the vent versus time for a constant mass flow rate release of 390 g/s in a 30 m^3 enclosure with a 20 cm by 20 cm vent.

It can be stated that the pressure peaking effect only occurs during the injection of a lighter gas, e.g. hydrogen, into a heavier gas, e.g. air. In the beginning of the process $M_{encl} \gg M_h$. While the above analysis relates to a constant mass flow rate of release the analysis is also applicable in the case of blow down. However, the maximum overpressure will be reduced. This can be explained by considering Equation 5 in the case of blow down $\frac{\dot{m}^t_{nozz}}{M_h}$ will not be a constant as $\dot{m}^t_{nozz}$ will be continuously decreasing. Thus the point at which $\frac{\dot{m}^t_{nozz}}{M_h} = \frac{\dot{m}^t_{vent}}{M_{encl}}$ will occur at a lower value of $\frac{\dot{m}^t_{vent}}{M_{encl}}$, i.e. earlier on the pressure-time dependence.

3.3. Maximum overpressure for the case of a constant mass flow rate leak

As discussed in the previous section the maximum enclosure pressure occurs at the point when there is a maximum number of moles in the enclosure i.e. when $\frac{\dot{m}^t_{nozz}}{M_h} = \frac{\dot{m}^t_{vent}}{M_{encl}}$. In the case of a constant $\dot{m}^t_{nozz}$ i.e. no blow down then for a given vent area *A* the maximum number of moles will always occur at the same ratio of $\frac{\dot{m}^t_{vent}}{M_{encl}}$, and hence values of $\dot{m}^t_{vent}$ and M_{encl} and therefore ρ_{encl}. Thus, the maximum overpressure P_{max} which occurs at $t = t(P_{max})$ is independent of enclosure volume for the scenario of a constant $\dot{m}^t_{nozz}$ i.e.:

$$P_{max} = \frac{\rho^{t(P_{max})}_{encl} RT}{M^{t(P_{max})}_{encl}}. \quad (8)$$

However, the time at which P_{max} occurs is dependent on enclosure volume for a constant mass flow rate $\dot{m}^t_{nozz}$ and vent(s) area *A*. The larger the enclosure volume, the longer it will take to reach $M^{t(P_{max})}_{encl}$ and hence P_{max}. This is demonstrated in Fig. 5 where overpressure versus time for a constant mass flow rate release of 390 g/s is compared for 3 different enclosure volumes with a 20x20 cm vent.

Figure 5. Overpressure versus time for a constant mass flow rate release of 390 g/s into enclosure volumes of 10 m^3, 30 m^3 and 100 m^3 with a 20x20 cm vent.

In the case of a constant $\dot{m}_{nozz}^{t}$ it is known that at $t = t(P_{max})$ the following relationships apply (please note in Equations 9 to 14, it is assumed the values of ρ_{encl}, M_{encl} and *Y* are the values at $t = t(P_{max})$, this superscript has been omitted for clarity).

From the ideal gas law it follows that:

$$\Delta P_{max} = \frac{\rho_{encl} RT}{M_{encl}} - P_0, \tag{9}$$

From Equation 5 it follows that at $t = t(P_{max})$,

$$\frac{\dot{m}_{nozz}^{t}}{M_h} = \frac{\dot{m}_{vent}^{t}}{M_{encl}} = \frac{\rho_{encl} vA}{M_{encl}}, \tag{10}$$

In Equation 10 velocity, v can be rewritten to give:

$$\frac{\dot{m}_{nozz}^{t}}{M_h} = \frac{\rho_{ence} A}{M_{encl}} \sqrt{\frac{2\Delta P_{max}}{\rho_{encl}}}, \tag{11}$$

Rearranging Equation 11 gives an expression for ΔP_{max}

$$\Delta P_{max} = \frac{\left(\left[\frac{\dot{m}_{nozz}}{M_h A}\right] M_{encl}\right)^2}{2\rho_{encl}}. \tag{12}$$

Equations 9 and 12 represent two different equations for ΔP_{max} hence it follows that:

$$\frac{\rho_{encl} RT}{M_{encl}} - P_0 = \frac{\left(\left[\frac{\dot{m}_{nozz}}{M_h A}\right] M_{encl}\right)^2}{2\rho_{encl}} \tag{13}$$

The purpose of this exercise is to determine ΔP_{max}however; Equation 13 cannot be solved directly because there are two unknowns, M_{encl} and ρ_{encl} . In order to progress it is necessary to express both M_{encl} and ρ_{encl} in terms of either mass fraction *Y* or mole fraction *X* of hydrogen. The example of mass fraction *Y* is described here (*X* was found to be more complicated)

Molecular mass of the mixture in the enclosure can be written it terms of mass fractions of gas and air as

$$M_{encl} = \frac{M_h M_a}{YM_a + (1-Y)M_h}. \tag{14}$$

Similarly density can be written in terms of mass fraction of hydrogen, *Y*, as

$$\rho_{encl} = \{Y\rho_h + (1-Y)\rho_a\}. \tag{15}$$

We can now substitute Equations 14 and 15 into Equation 13

$$\frac{\{Y\rho_h + (1-Y)\rho_a\} RT}{\left(\frac{M_h M_a}{YM_a + (1-Y)M_h}\right)} - P_0 = \frac{\left(\left[\frac{\dot{m}_{nozz}}{M_h A}\right] \frac{M_h M_a}{YM_a + (1-Y)M_h}\right)^2}{2\{Y\rho_h + (1-Y)\rho_a\}} \tag{16}$$

The equation set (14, 15 and 16) represents three equations and three unknowns i.e. *Y*, M_{encl} and ρ_{encl} and thus can be solved algebraically with an appropriate numerical tool at this point. However, Equation 9 has been expanded in order to develop a single algebraic relationship for ΔP_{max}. Equation 9 can be written in terms of *Y* as follows

$$\Delta P_{max} = \frac{(YM_{a+}(1-Y)M_h)\{Y\rho_h+(1-Y)\rho_a\}RT}{M_h M_a} - P_0. \quad (17)$$

Each term within Equation 17 can be expanded, and the result is a quadratic equation in terms of the mass fraction *Y*. The equation takes the form $dY^2 + bY + c = 0$ and thus it is possible to solve for *Y* using the well-known relationship given in Equation 18.

$$Y = \frac{-b \pm \sqrt{b^2 - 4dc}}{2d} \quad (18)$$

where

$$d = (RT)(M_a\rho_h - M_a\rho_a - M_h\rho_h + M_h\rho_a), \quad (19)$$

$$b = [(RT)(M_a\,\rho_a + M_h\rho_h - 2M_h\rho_a)] \quad (20)$$

$$c = RTM_h\rho_a - M_h M_a P_0 - M_h M_a \Delta P_{max} \quad (21)$$

Note that analysis of a wide range of scenarios lead to the conclusion that for hydrogen in air the value of *Y* is always equal to the solution whereby the square root term is subtracted

Equation 11 can be rewritten in terms of *Y* to give:

$$\dot{m}_{nozz} = \frac{M_h\{Y\rho_h + (1-Y)\rho_a\}\{YM_{a+}(1-Y)M_h\}A}{M_h M_a}\sqrt{\frac{2\Delta P_{max}}{\{Y\rho_h + (1-Y)\rho_a\}}} \quad (22)$$

Equation 18 can be substituted for *Y* in Equation 22 resulting in an equation relating maximum overpressure to mass flow rate. This can be used to estimate either maximum vent area or leak flow rate for a fixed overpressure, e.g. overpressure that an enclosure can withstand.

The equations presented are in terms of hydrogen and air but may be applied to any gas mixture. In order to solve for a hydrogen-air scenario the following values can be substituted into Equation 18: M_a = 0.02897 kg, M_h = 0.002 kg, ρ_a=1.2 kg/m^3, ρ_h=0.0848 kg/m^3, P_0 =101325 Pa, T=293 K and *R*= 8.314472. It is acknowledged that these values correspond to ambient conditions for pressure and temperature, however, they provide indicative values. For hydrogen air scenarios Equation 24 applies and can be substituted into Eq. 23 for leak rate:

$$Y = \frac{73.43 - \sqrt{5384.96 - 0.016917\Delta P_{max})}}{145.991} \quad (23)$$

Thus for a selected maximum overpressure it is possible to calculate hydrogen mole fraction, *Y*, at which this ΔP_{max} occurs from Equations (18-21) (simplified to Eq. 23 if hydrogen and air) and then substitute this value into equation 22 to solve for vent area or leak rate depending on the variable of interest. Note that the dimensions of ΔP_{max} are Pascals.

3.3. The nomogram (constant mass flow rate)

There is a need for tools which can be easily used by hydrogen safety engineers and/or regulators permitting these technologies. Therefore, the nomogram presented in Fig. 6 has been developed to enable the easy graphical calculation of overpressure in an enclosure for the case of a sustained (constant mass flow rate) release as a conservative approach compared to a blow down release. Whilst it should be emphasised that a constant mass flow rate represents a conservative case, the authors have found that in the case where overpressures are likely to be prohibitive (i.e. high-pressure release, minimum ventilation) then a maximum pressure is reached within a matter of seconds, before leak rate is significantly reduced. The reader is referred to the more detailed analytical model for comparison in cases where a less conservative approach is desirable.

The nomogram is independent of enclosure volume as described in the previous section. The lower part of the nomogram was developed using the under-expanded jet theory [9]. Storage pressure versus mass flow rate has been calculated for a series of leak diameters. Diameters from 0.1 mm to 25 mm have been considered and pressures in the range 0.2–100 MPa, this range was deemed to be sufficiently representative of current applications. Enclosure temperature was assumed to be a constant in the calculations equal to 288 K.

The upper part of the graph enables the calculation of overpressure for a range of vent areas. The vent areas chosen lead to overpressures in the range approximately 1-100 kPa. For cases outside this range, or a more accurate estimation, direct application of the equations (18-22) outlined in the previous section is recommended.

To use the nomogram start with the y axis on the lower half of the graph and select storage pressure, read across horizontally to the leak diameter, see the example of 35 MPa, 5 mm in Fig. 6. Read vertically upwards to calculate the mass flow rate of the leak (in the example this is 0.39 kg/s). Continue vertically upward from the mass flow rate to the point of intersection with the line for the required vent area. In Fig. 6 two ventilation areas are selected to highlight the difference in the resulting overpressure for the same leak rate. In Example 1 (E1) a leak area of 0.1 m^2 is selected, reading across, horizontally to the left and the point of intersection with the *y* axis represents the overpressure in the enclosure, for E1 a value of approximately 3 kPa is predicted. In E2 a vent area of 0.01 m^2 is selected, (this is slightly less than that of a typical brick which is 0.0125m^2), the overpressure predicted for this smaller area is 70 kPa, a value sufficient to cause considerable structural damage. E1 and E2 emphasise the difference vent area can make to a “safe” or “unsafe” scenario.

Figure 6. Nomogram to estimate maximum overpressure in an enclosure for a known storage pressure, leak diameter and vent area (constant mass flow rate of a leak scenario).

3.4 Hydrogen concentration and overpressure

In the case of a constant mass flow rate leak it has been shown that for a given vent area and leak rate the maximum overpressure will occur at the same mole fraction of hydrogen regardless of the enclosure volume (Equations 17). In the case of a constant leak rate the mole fraction of hydrogen will increase from 0 to 1 as the leak progresses. However, it is important to note that the mole fraction of hydrogen in the enclosure at the point of maximum overpressure varies with both leak rate and vent area (Equation 12).

For a given constant mass flow rate of hydrogen a decrease in vent area will mean a higher overpressure in the volume but the point of maximum overpressure will occur at a lower hydrogen concentration. Similarly an increase in vent area will mean a lower maximum overpressure, however, the mole fraction of hydrogen will increase more rapidly and the concentration of hydrogen in air at the point of maximum overpressure will increase. A larger vent area may reduce the risk of excessive overpressures but it will mean that hydrogen

concentration levels grow more rapidly in the enclosure. Figure 7 illustrates the effect of vent size on overpressure and hydrogen concentration dynamics for a constant leak rate (1 g/s) in a 1 m^3 enclosure. It can be seen from Fig. 7 how the peak in overpressure occurs sooner and is of a lower magnitude for a greater vent area. The concentration dynamics are almost identical for the vent areas of 0.001 m^2 and 0.0005 m^2, the difference becomes more pronounced as the vent area is decreased to 0.0001 m^2 where it can be seen how with decreasing vent size it takes longer to reach a given concentration within the enclosure for the same leak rate.

Figure 7. Overpressure and concentration versus time for a constant mass flow rate release of 1 g/s into an enclosure volume of 1 m^3 for vent areas of 0.0001, 0.0005 and 0.001 m^2.

In recent work [1] a simple formula was presented for scenarios where a leak mass flow rate in an enclosure will eventually lead to a volumetric hydrogen concentration of 100% after some time. The formula [1] is reproduced below (Equation 24), where *h* is the vent height,

$$\dot{m}_h > A\sqrt{h}C\sqrt{\frac{8g\rho_{encl}(\rho_{atm}-\rho_{encl})}{9}}. \quad (24)$$

Equation 24 relates vent height and width and lower limit of hydrogen leak mass flow rate for scenarios where 100% hydrogen (vol.) will be reached in an enclosure, it is demonstrated in [1] that C = 0.6 has to be used. The model [1] assumes there is no air ingress, thus the vent size predicted is the maximum allowable to ensure the volume will eventually reach a concentration of 100% hydrogen, or the mass flow rate is at its lower limit. Equation 24 can be used to estimate the vent size for a given leak rate which will eventually lead to 100% hydrogen concentration in the enclosure. This vent size and leak rate can then be used as inputs to the model for the pressure peaking phenomenon in order to estimate the time it takes to reach a given hydrogen concentration and value of the peak. It has to be emphasised that the present model for pressure peaking phenomenon can be applied only when the condition of Equation 24 is satisfied. In a real leak scenario the hydrogen mass flow rate at the nozzle will decrease and a situation may eventually arise whereby there is bidirectional flow across the vent, at this point Equation 24 does not apply and pressure peaking will not occur. Pressure peaking occurs only during the initial stages of a release when there is no air ingress. Whilst a large nozzle may result in bi directional flow more quickly, the maximum overpressure is proportional to mass flow rate. Hence, whilst a smaller diameter nozzle may result in a longer period before air ingress occurs, the resultant maximum over pressure will be lower leading to less potential damage.

A nomogram was created based on these steps which enable calculation of the time to reach a concentration of 90% (vol.) of hydrogen in enclosure for particular enclosure volume, vent size and leak rate. The nomogram is presented in Fig. 8. To use the nomogram select the hydrogen leak rate and read horizontally across until intersecting with the diagonal line, reading vertically up from the point of intersection will give the maximum vent area which will ensure that a concentration of 100% hydrogen will be reached in the enclosure i.e. the maximum vent area at which all flow will be out of the enclosure and there will never be air ingress. From the vent area read vertically up until intersecting with the diagonal line which represents the volume of interest read horizontally to the y axis to determine the time to a concentration of 90%.

Figure 8. Nomogram to estimate the time to reach 90% vol, hydrogen concentration in an enclosure where the vent and leak combination is such that all flow is out of the enclosure.

3.5 Accounting for blow down (reduction of storage pressure and mass flow rate in time)

A varying mass flow rate release will mean that the phenomenological model cannot be simplified and the volume of the enclosure will have an effect on the maximum overpressure. A constant mass flow rate release represents a worst case "conservative" scenario. In the case of blow down i.e. a reducing leak rate, then the maximum overpressure will be lower in the enclosure.

The model [9] was used to simulate blow down of hydrogen from the storage tank. This model takes into account the under-expanded jet theory given in the same book [9] and can be used to calculate decay of pressure and mass flow rate during a release from a storage tank of known volume through an orifice of known diameter. The heat transfer during blow down was not accounted for; an isothermal approach which assumed a temperature of 288 K was used based on available experimental data for blow downs at such pressures through pipelines of similar size. For a given diameter, storage pressure, and hydrogen inventory, the output of the blow down model (changing mass flow rate) was used as an input to the phenomenological model to predict overpressure in a garage with a known volume and vent size.

Figure 9 gives the overpressure dynamics for a the case of a constant mass flow rate release and blow down of 4.75 kg of hydrogen at initial pressure 35 MPa through a 5.08 mm diameter orifice into an enclosures of 30 m^3 and 10 m^3 with a vent size of 20 cm by 20 cm. Note as the inventory of hydrogen is increased the pressure dynamics curve for a blow down scenario becomes closer to that for a constant mass flow rate release.

Figure 9. Overpressure versus time for a constant mass flow rate from 350 bar storage through a 5.08 mm orifice (390 g/s), and blow down from 4.75 kg at 35 MPa through a 5.08 mm orifice into enclosure volumes of 10 m^3 and 30 $m^3$with a 20 cm by 20 cm vent.

4.0 Model validation

The prediction of pressure dynamics by the phenomenological model was compared with CFD simulations in [6] for a constant mass flow rate release. It was demonstrated in [6] that when value of *C=0.6* was used the model and CFD showed good agreement, *0.6* was chosen as a typical value from the literature [13] and the CFD and model predictions matched exactly for *C=0.55* as illustrated in Fig. 10. The phenomenon was recently validated experimentally [8] for laboratory scale experiments where the phenomenological model reproduced closely the experimental pressure dynamics for three different gases (air, hydrogen and helium). To date, the author is not aware of any larger scale experiments performed specifically to validate the pressure peaking phenomenon. However, previous experimental work, not intended for this purpose has also shown evidence of the pressure peaking phenomenon and thus efforts have been made to compare this data as outlined in the following section.

Figure 10. Overpressure versus time for a constant mass flow rate from 350 bar storage through a 5.08 mm orifice (390 g/s) in a 30.4 m^3 enclosure with a 25 cm by 5 cm vent, CFD and phenomenological model.

Work by Ekoto et al [2] describes experiments of release, dispersion, and combustion within a scaled test facility representative of a release from a forklift within an enclosed space. Whilst analysis of the overpressure data presented in [2] is primarily focused on combustion phenomena, overpressures are also presented for the initial unignited stage of the release. Indeed it is noted in [2] how "The initial 1 kPa pressure rise that occurred before ignition was attributed to the expansion of the released H_2". The overpressure data in this early stage has been compared in this work with pressure predicted by the phenomenological model for pressure peaking.

In the experiments described in [2] 0.0363 kg of compressed hydrogen stored at approximately 13.7 MPa was released through a orifice of diameter 3.46 mm from a forklift model into a scaled warehouse type enclosure and ignited after a short delay. The test facility measured LxWxH =3.64 m x 4.59m x 2.72 m, total internal volume 45.4 m^3. The warehouse contained a forklift model of dimensions LxWxH= 34.3 cm x 34.3 cm x 43.5 cm high, volume of the forklift is equal to 0.0512 m^3. An air leakage test was performed in [2] in order to estimate total leak area. For test 8 and 9 described in [2] the calculated leakage area was 60 cm^2 and for tests 12 and 13 the calculated leakage area was 36.8 cm^2.

In order to compare the experimental results in [2] with the pressure peaking model the leak rate was estimated. In order to do this the blow down model [9] was applied to calculate mass flow rate. This was then used as an input to the phenomenological model, along with the free volume and the vent sizes in order to estimate overpressure.

It should be noted that an isothermal blow down model was used as the phenomenological model assumes the system is isothermal. However, experimental results presented by Schefer et al. [14] for blow down from 43.1 MPa through a 5.08 mm orifice demonstrated a steady decrease in stagnation chamber temperature (to -45˚C) over the first 100 s of their release, and a significant decrease and fluctuation was noted in the first 2 seconds of their release (a decrease from ambient to under -5˚C occurred in < 1s, this then increased to > 0˚C by 2 s before dropping steadily as mentioned). The work presented here is focused on the first 2 s of the release presented in [2], thus it is extremely likely that there are significant changes in the stagnation temperature over the period considered, this can clearly be seen in [14]. A simple adiabatic expansion calculation for the release in [2] predicts a stagnation temperature drop to 72 K; however in reality heat transfer will result in a less significant temperature drop. Data cited in [15] notes stagnation temperatures as low as 80 K have been observed following blow down from a hydrogen storage system. With this in mind, several stagnation temperatures were used as an input to the isothermal blow down model. The resulting mass flow rate was used as an input to the pressure peaking model and indeed the predicted overpressure was found to be sensitive to the stagnation temperature considered. Stagnation temperatures of -5 ˚C and - 45˚C were considered based on the data in [14], a value of -193˚C was also checked [15] for reference purposes. The pressure dynamics predicted using a value of -193˚C in the blow down model is not shown here, the overpressure predicted was significantly higher (200%) than that observed experimentally due to the over prediction of the mass flow rate. The authors acknowledge that beyond the initial stages of the release an isentropic modelling approach may be more realistic, however, an isothermal approach was deemed to be appropriate to represent the initial seconds of the release, and an isentropic approach will predict a temperature tending towards 0K which is not realistic. It is also worth noting that there was limited data available at the time of the study to further investigate the most appropriate approach.

A comparison of the overpressure predicted using the phenomenological model with stagnation temperatures of -5˚C and - 45˚C , and the experimental data is given in Figs. 11 and 12 for tests 8/9 and 12/13 respectively.

Figure 11. Overpressure versus time a comparison of modelled and measured values for tests 8/9.

Figure 12. Overpressure versus time a comparison of modelled and measured values for tests 12/13.

Figures 11 and 12 clearly demonstrate the sensitivity of the model predictions to choice of stagnation temperature. However, it can be seen how for a stagnation temperature of - 45˚C how the modelled pressure dynamics exhibit the same behaviour as the experimental values. The modelled overpressure under-predicts that measured experimentally by approximately 10% in each case. As mentioned, a number of assumptions have been made in the application of the model including estimation of mass flow rate decay, *C* (taken as 0.55 [7]) and the total vent area. In addition it is not possible to estimate the contribution of any cumulative error in the blow down model combined with that in the pressure peaking methodology. As mentioned at the absence of appropriate experimental data means it is not possible to investigate this further. Indeed a need exists for experimental data for blowdown scenarios, previous simulation work performed by the authors [7] has focused on blowdown scenarios and highlights the safety concerns.

5.0 Summary and Conclusions

The unforeseen physical phenomena of pressure peaking has been described and explained. This phenomenon occurs for hydrogen releases in enclosures where the vent(s), volume, and leak rate are such that there will be no air ingress to the enclosure. It should be noted that the phenomena is more pronounced for hydrogen than any other combustible gas and is also notable with helium. The overpressures which may result can be capable of structural damage.

Two methods to estimate overpressure in an enclosure with vent(s) are presented, both a simplified and more complex means.

For the case of a constant mass flow rate release, it is demonstrated how the maximum overpressure may be expressed as a function of the hydrogen mass fraction only and is independent of enclosure volume. The hydrogen mass fraction can be solved for and subsequently used to determine maximum overpressure. An expression relating leak rate, hydrogen mass fraction and maximum overpressure is given, thus enabling the maximum overpressure to be calculated for a known leak rate or vice versa. These reduced analytical equations are for the case of a constant leak rate only. A nomogram is presented for the case of a sustained leak. This nomogram can be used to estimate maximum overpressure in the enclosure and is based on vent area and leak rate. Where pressure dynamics are of interest a system of equations is presented.

Work [1] has been drawn upon to create a second nomogram allowing calculation at which the hydrogen concentration in an enclosure will reach 90% vol. This nomogram is a function of leak rate and volume. The vent areas are calculated as the maximum values which will ensure that there is no air ingress to the enclosure.

Experimental evidence of the phenomenon is shown.

Pressure peaking is relevant to the use of hydrogen and fuel cell systems indoors and should be accounted for in system design. Whenever a hydrogen release occurs in a vented enclosure where the release is sufficient to ensure no air ingress the effect is present. However, the amplitude, rate and duration vary depending on the conditions. Thus, this dynamic pressure rise which is most pronounced for a release of hydrogen within a ventilated enclosure should be accounted for when performing safety engineering for indoor use of hydrogen and fuel cell systems. It is clear from the examples shown that the overpressures encountered in typical scenarios may be sufficient to cause significant structural damage. It should be emphasized that pressure peaking for the case of an *unignited* release is described here. Ongoing investigations into hydrogen fires in enclosures indicate that the overpressure will be significantly larger for the same release rate. Whilst the work presented here focuses primarily on constant mass flow rate scenarios, it has been shown [7] how pressure peaking is equally relevant in the case of blowdown and a need exists for experimental investigation.

6.0 Acknowledgments
The authors wish to thank Erik Merilo and Mark Groethe at SRI International for providing pressure data for the experiments described in [2].

7.0 References

1. Molkov V, Shentsov V, Quintiere J (2013), *Sustained Hydrogen Leak Concentration in Enclosure with One Vent*, Proc. of the 7th Intl Seminar on Fire and Explosion Hazards, 5-10 May 2013, Providence, R.I., USA, pp. 903-912.
2. Ekoto, I. W., Houf, W. G., Evans, G. H., Merilo, E. G., and Groethe, M. A. *Experimental investigation of hydrogen release and ignition from fuel cell powered forklifts in enclosed spaces*, International Journal of Hydrogen Energy (2012), Volume 37, Issue 22, November 2012, Pages 17446-17456.
3. Fuster, B, Houssin-Agbomson D., Jallais, S. et al. *Guidelines and recommendations for indoor use of fuel cells and hydrogen systems*, International Journal of Hydrogen Energy, Volume 42, Issue 11, 2017,Pages 7600-7607, https://doi.org/10.1016/j.ijhydene.2016.05.266.
4. Prasad K., Pitts W.M., Yang J.C. *A numerical study of the release and dispersion of a buoyant gas in partially confined spaces*, International Journal of Hydrogen Energy, Volume 36, Issue 8, April 2011, Pages 5200-5210.
5. Barley C.D., Gawlik K. *Buoyancy-driven ventilation of hydrogen from buildings: Laboratory test and model validation* International Journal of Hydrogen Energy, Volume 34, Issue 13, July 2009, Pages 5592-5603.
6. Brennan, S., Makarov, D. and Molkov, V., *Dynamics of Flammable Hydrogen-Air Mixture Formation in an Enclosure with a Single Vent*, Proceedings of the 6th International Seminar on Fire and Explosion Hazards, Research Publishing, July 2011, England, ISBN 978-981-08-7724-8.
7. Brennan S., Molkov V. *Safety assessment of unignited hydrogen discharge from onboard storage in garages with low levels of natural ventilation*. International Journal of Hydrogen Energy (2013), Volume 38, Issue 19, 27 June 2013, Pages 8159-8166.
8. Makarov, D., Shentsov, V., Kuznetsov, M., and Molkov, V. *Pressure peaking phenomenon: Model validation against unignited release and jet fire experiments* International Journal of Hydrogen Energy, Volume 43, Issue 19, 10 May 2018, Pages 9454-9469
9. Molkov V (2012) *Fundamentals of Hydrogen Safety Engineering, Part I*, www.bookboon.com, ISBN 978-87-403-0226-4.
10. Molkov, V., Makarov, D. and Bragin, M., *Physics and modelling of under-expanded jets and hydrogen dispersion in atmosphere*. Proceedings of the 24th International Conference on Interaction of Intense Energy Fluxes with Matter, Elbrus, Chernogolovka,, pp. 143-145 (2009).
11. Hess K, Leuckel W, Stoeckel A. *Formation of explosive clouds of gas on overhead release, and preventive measures*. Chemie-Ing. Techn, 45:323, 1973.
12. Lee's loss prevention in the process industries: hazard identification, assessment, and control, Volume 1. Elsevier. 2005 ISBN 0-7506-7555-1.
13. Emmons, D. D., *Vent flows*, SFPE Handbook, ed. P. J. Di Nenno, (2nd Edition), Society of Fire Protection Engineers, Boston, MA, USA., 1995.
14. Schefer, R.W. Houf, W.G. Williams, T.C. Bourne B., Colton J., *Characterization of high-pressure, underexpanded hydrogen-jet flames*, International Journal of Hydrogen Energy, Volume 32, Issue 12, August 2007, Pages 2081-2093.
15. Molkov V., and Saffers J.B., *Hydrogen jet flames*, International Journal of Hydrogen Energy, Volume 38, Issue 19, 27 June 2013, Pages 8141-8158

16. Brennan S., Hussein, H, Makarov D, Shentsov V., Molkov V. *Pressure Effects of an Ignited Release from Onboard Storage in a Garage with a Single Vent*, International Journal of Hydrogen Energy 2018 (accepted July 2017, in press)

Figure 1

Click here to download high resolution image

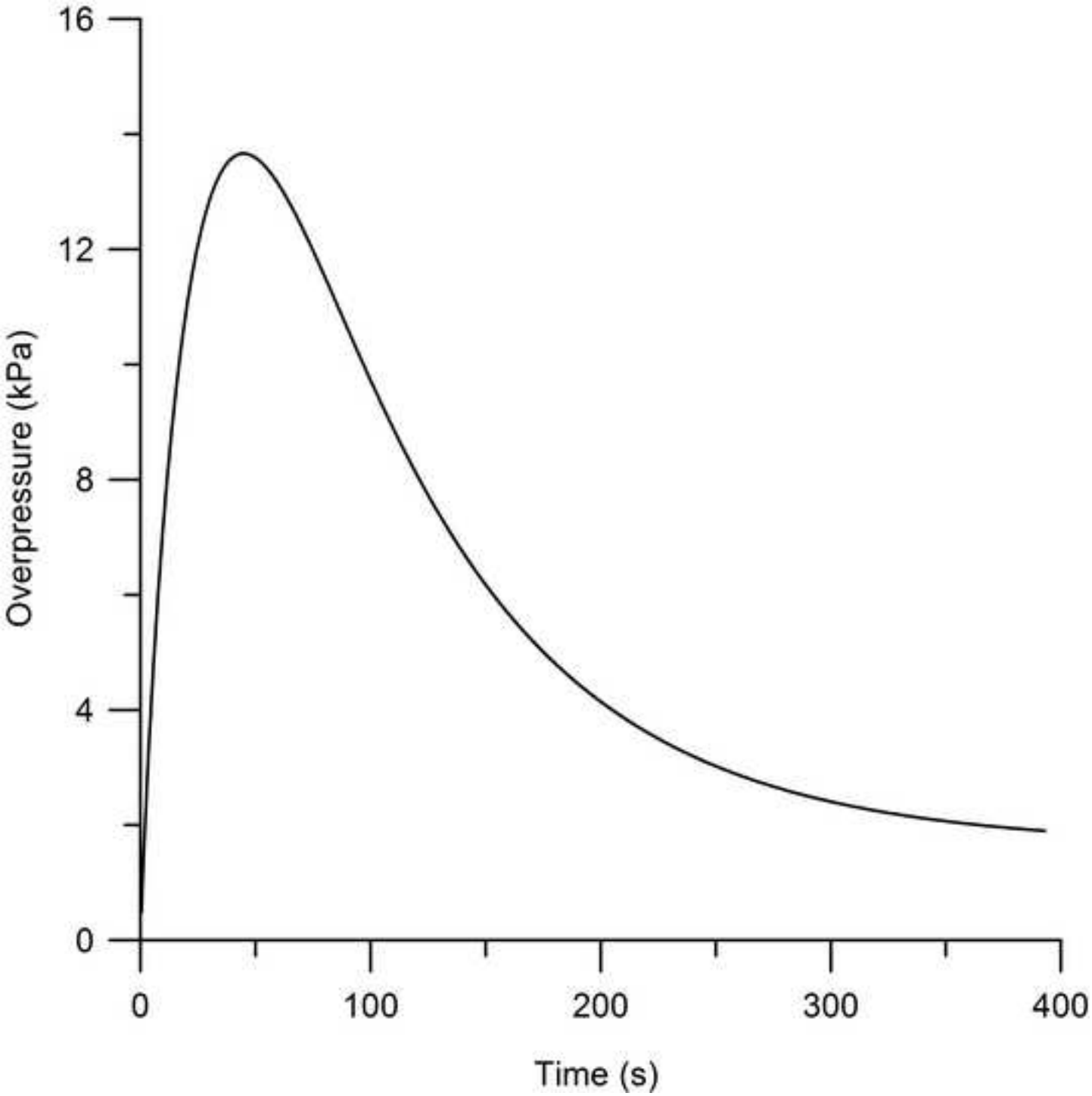

Figure 2

Click here to download high resolution image

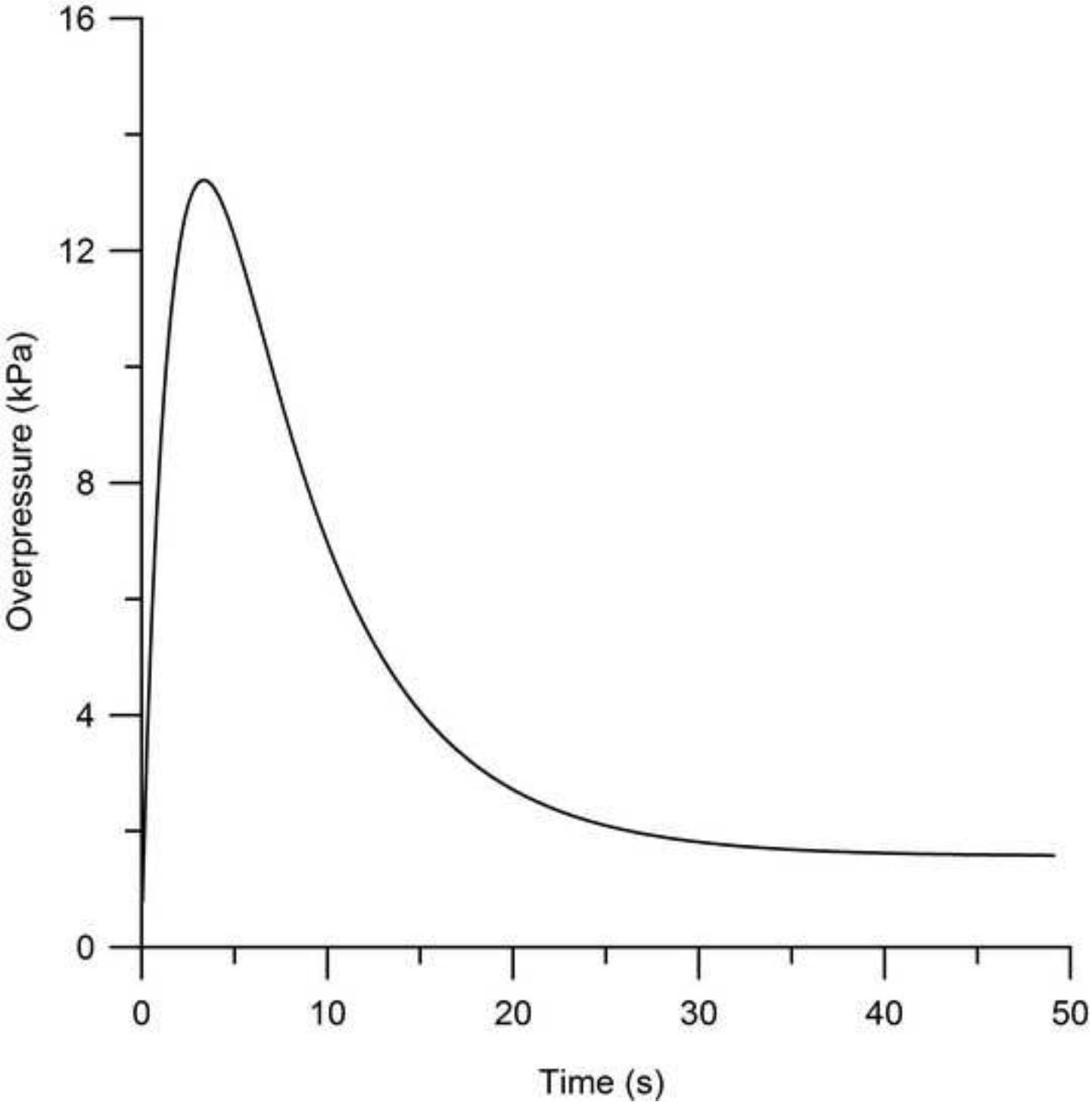

Figure 3

Click here to download high resolution image

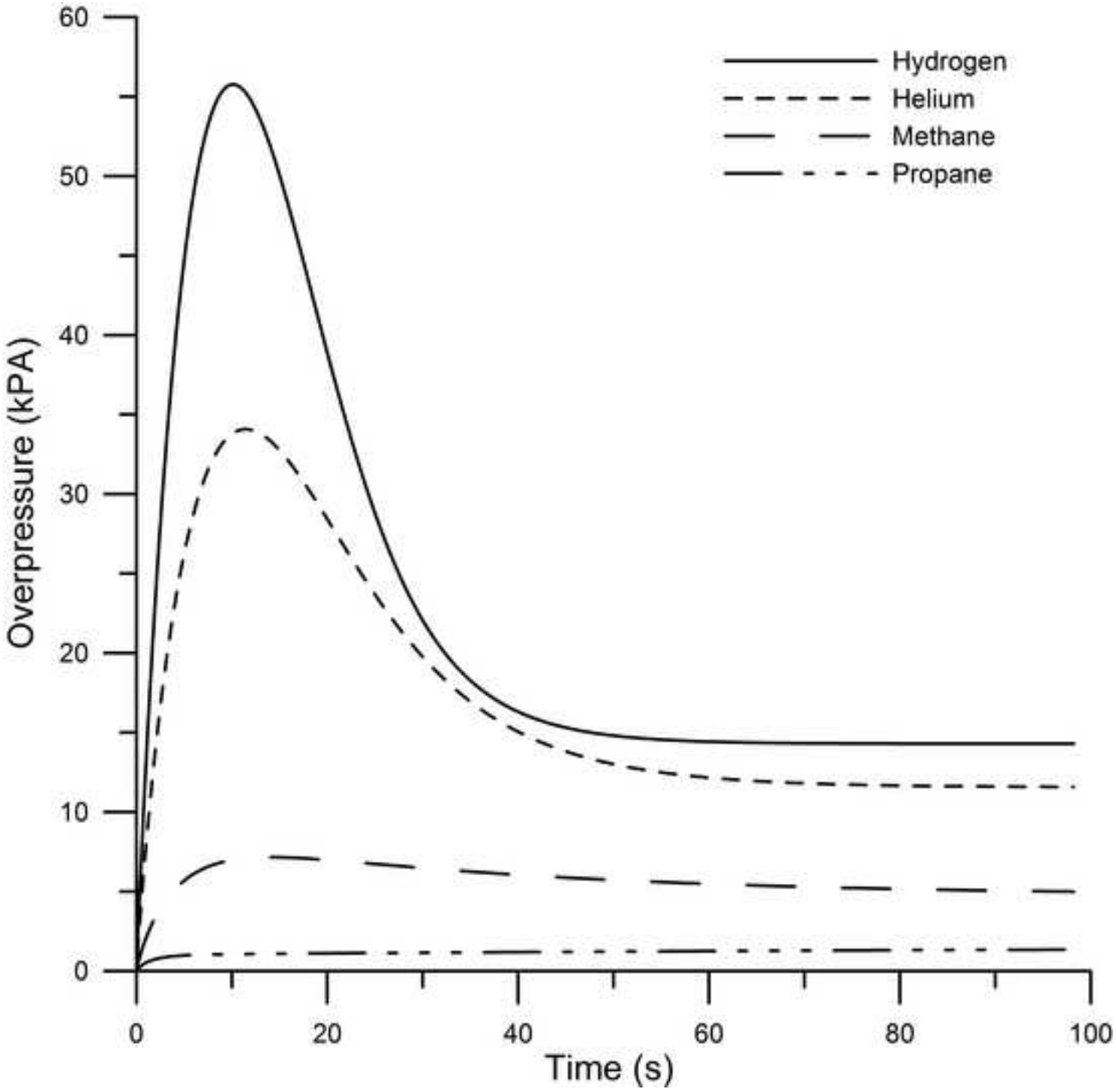

Figure 4

Click here to download high resolution image

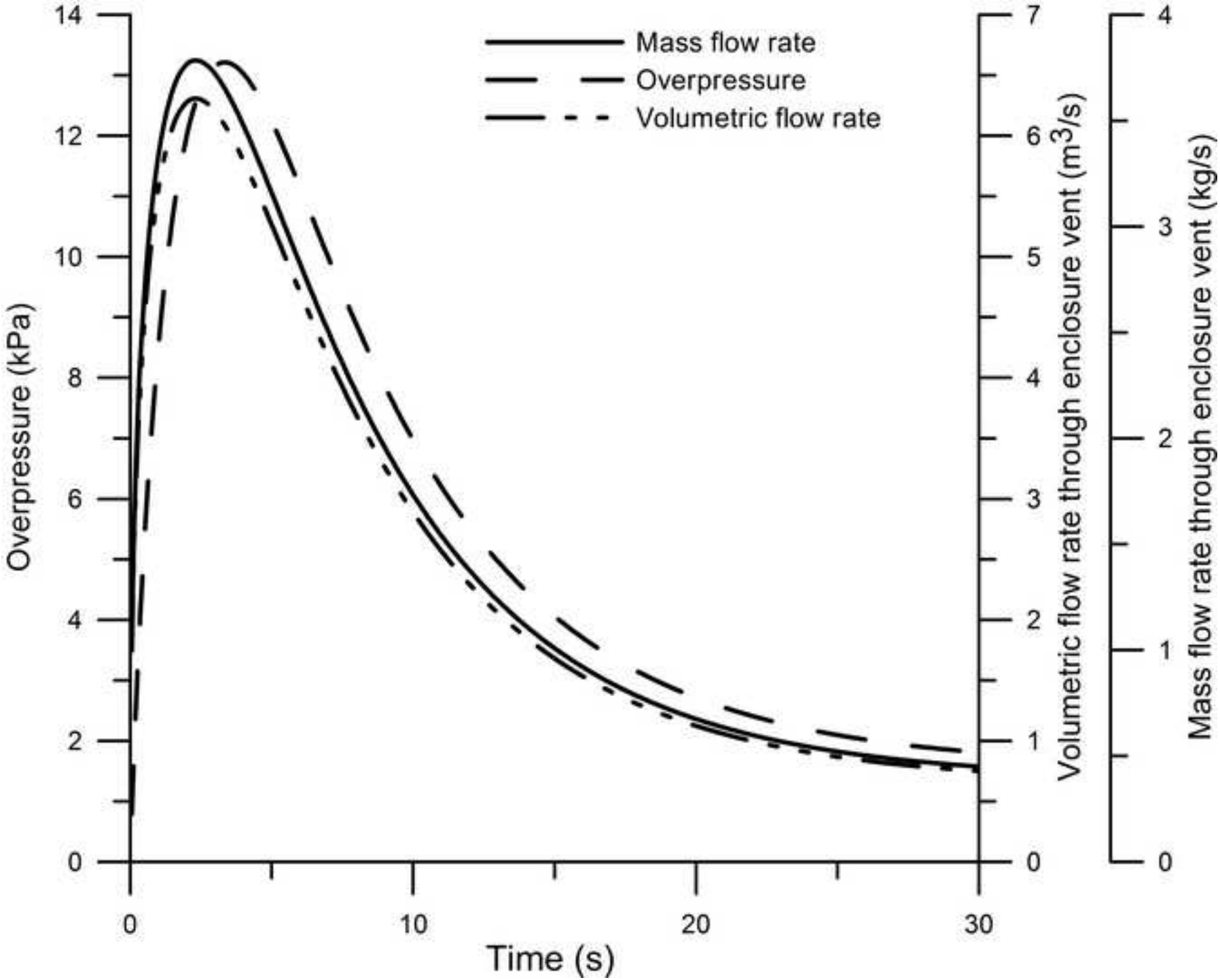

Figure 5

Click here to download high resolution image

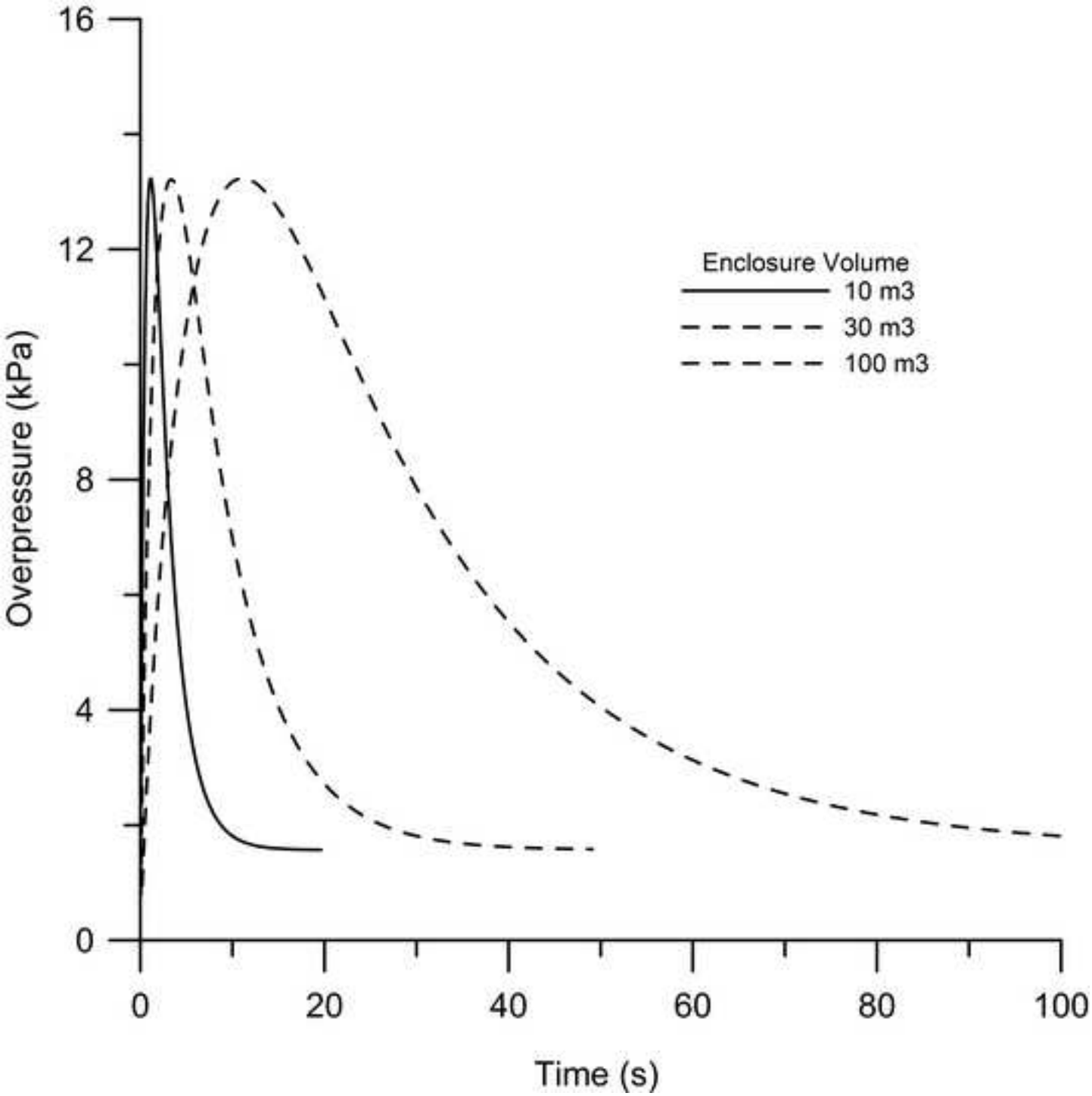

Figure 6
Click here to download high resolution image

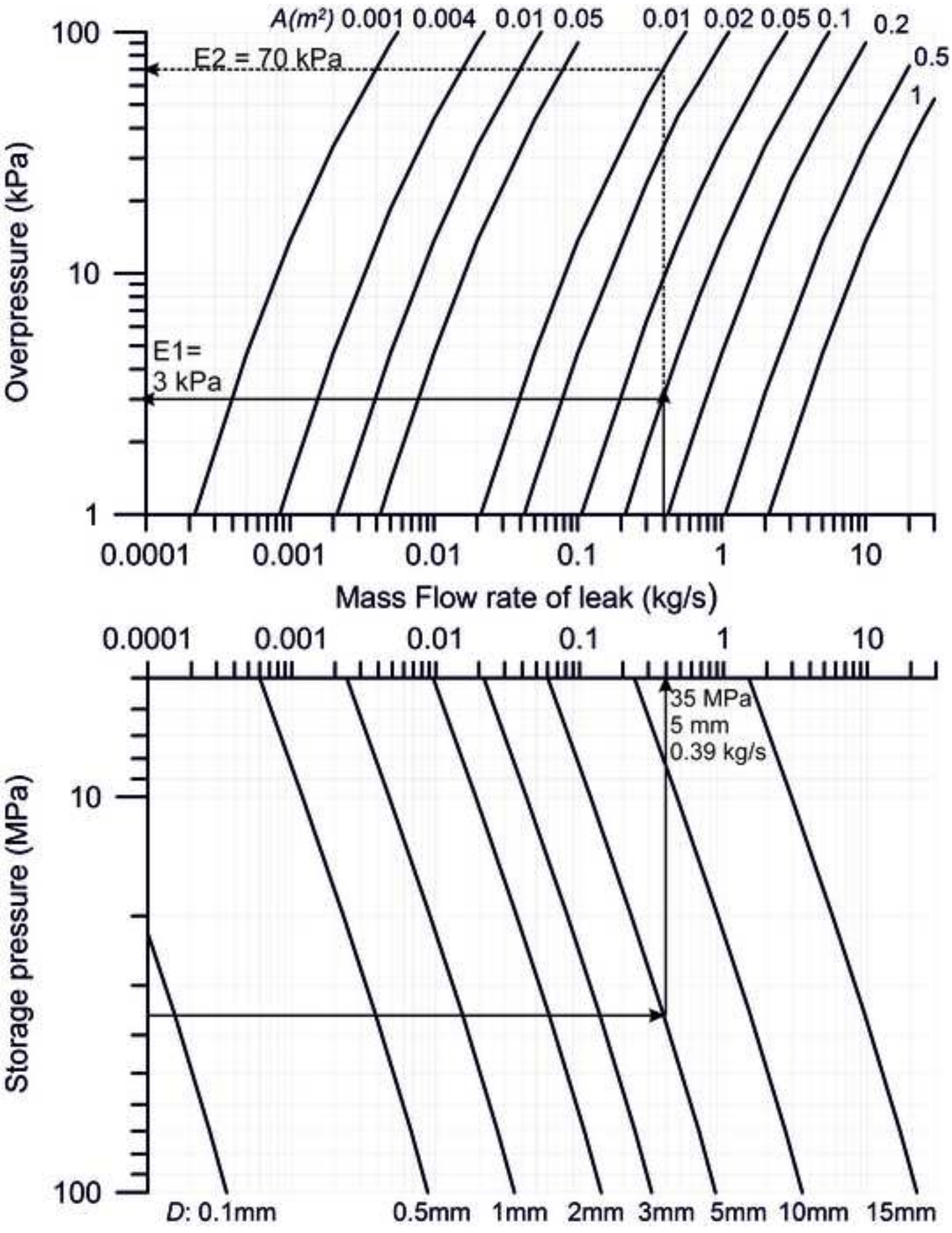

Figure 7

Click here to download high resolution image

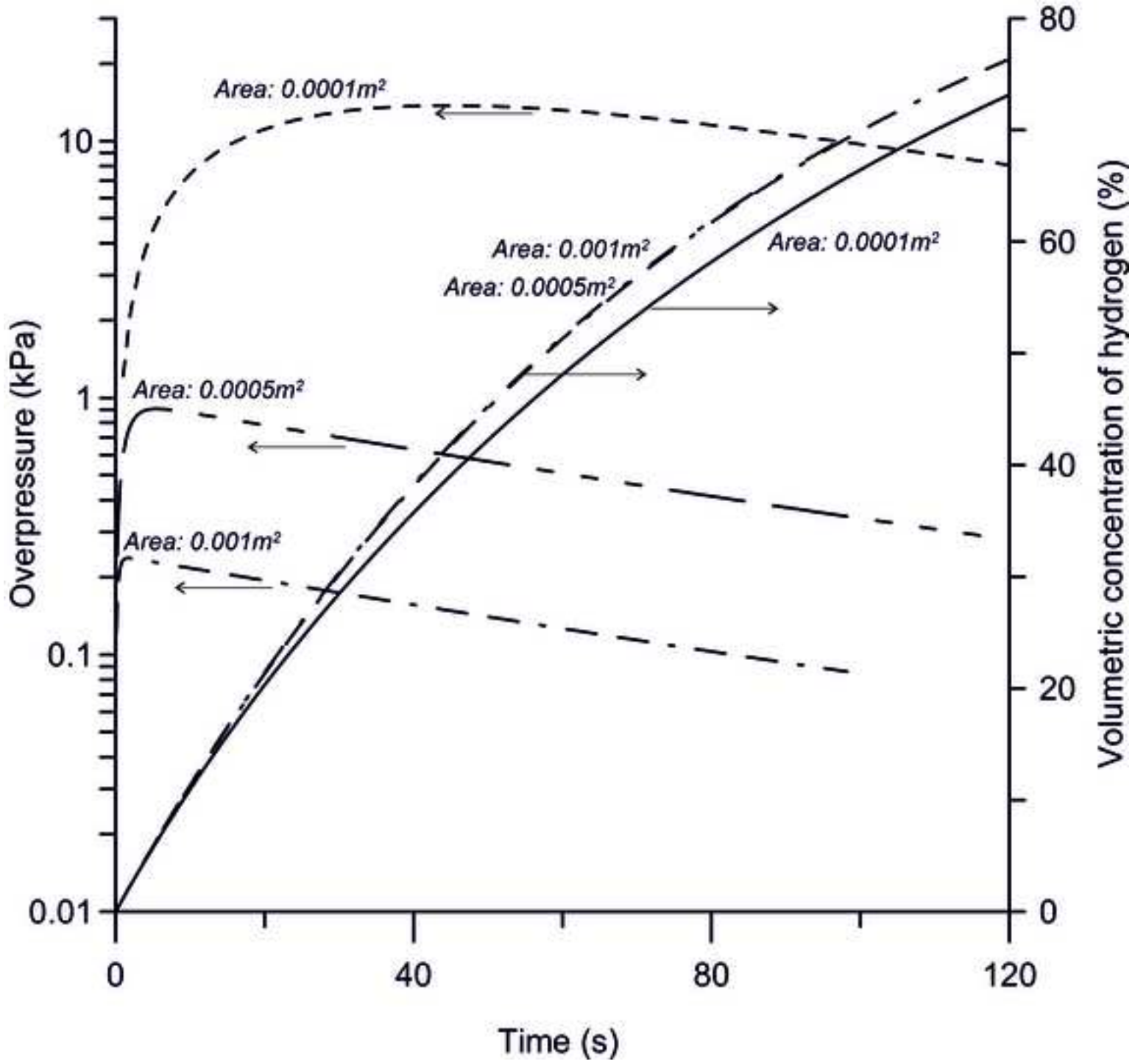

Figure 8

Click here to download high resolution image

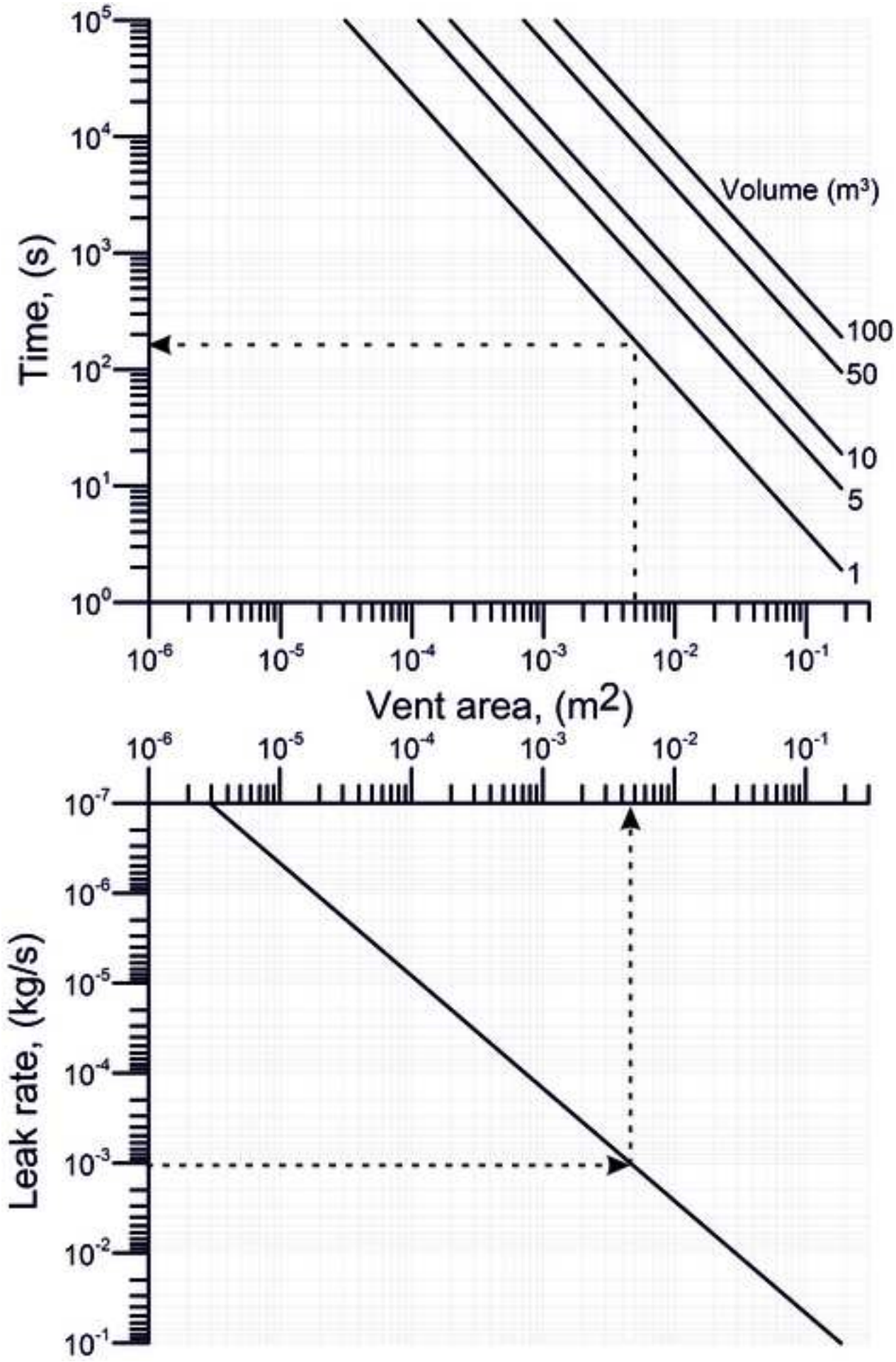

Figure 9

Click here to download high resolution image

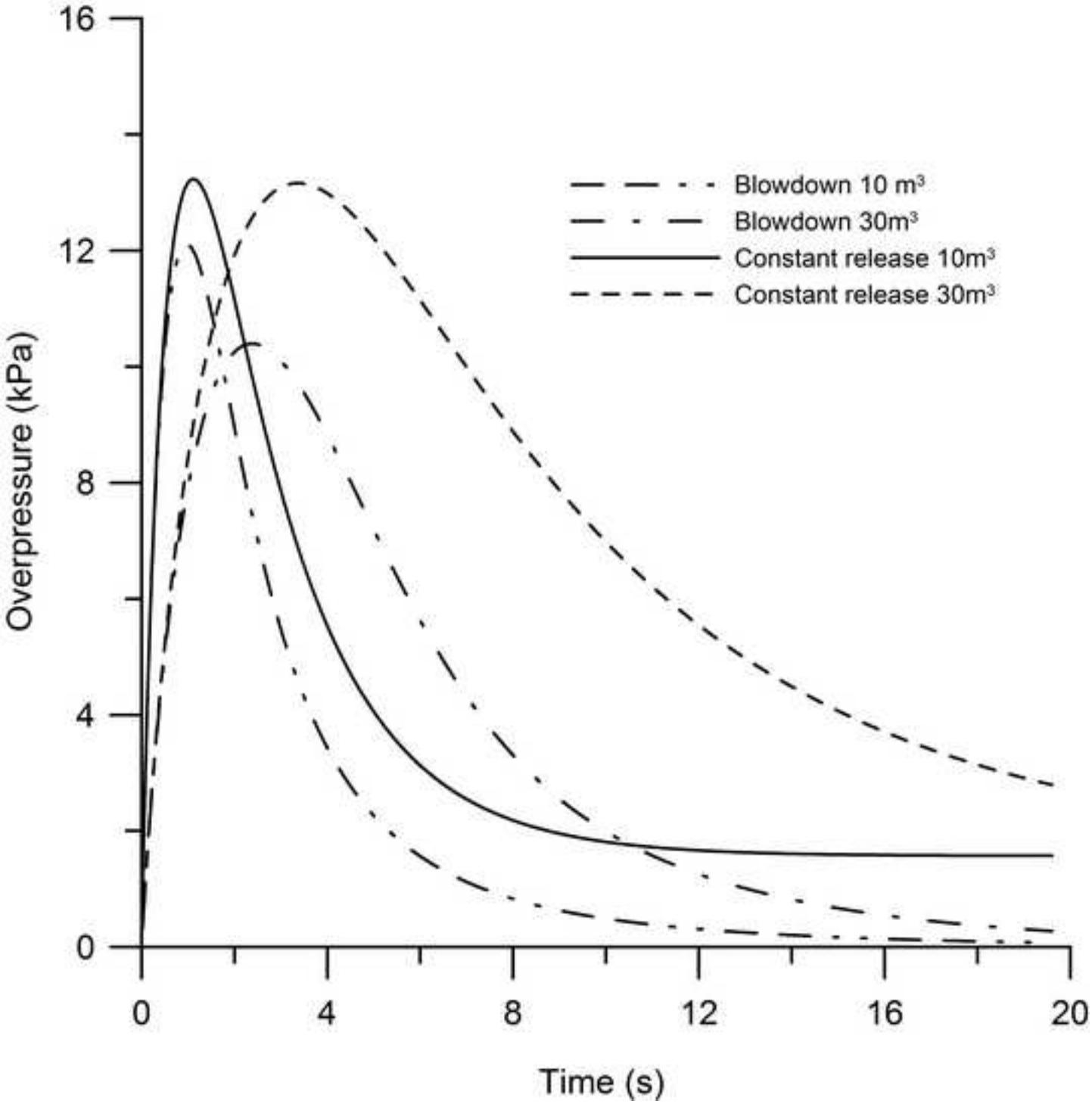

Figure 10

Click here to download high resolution image

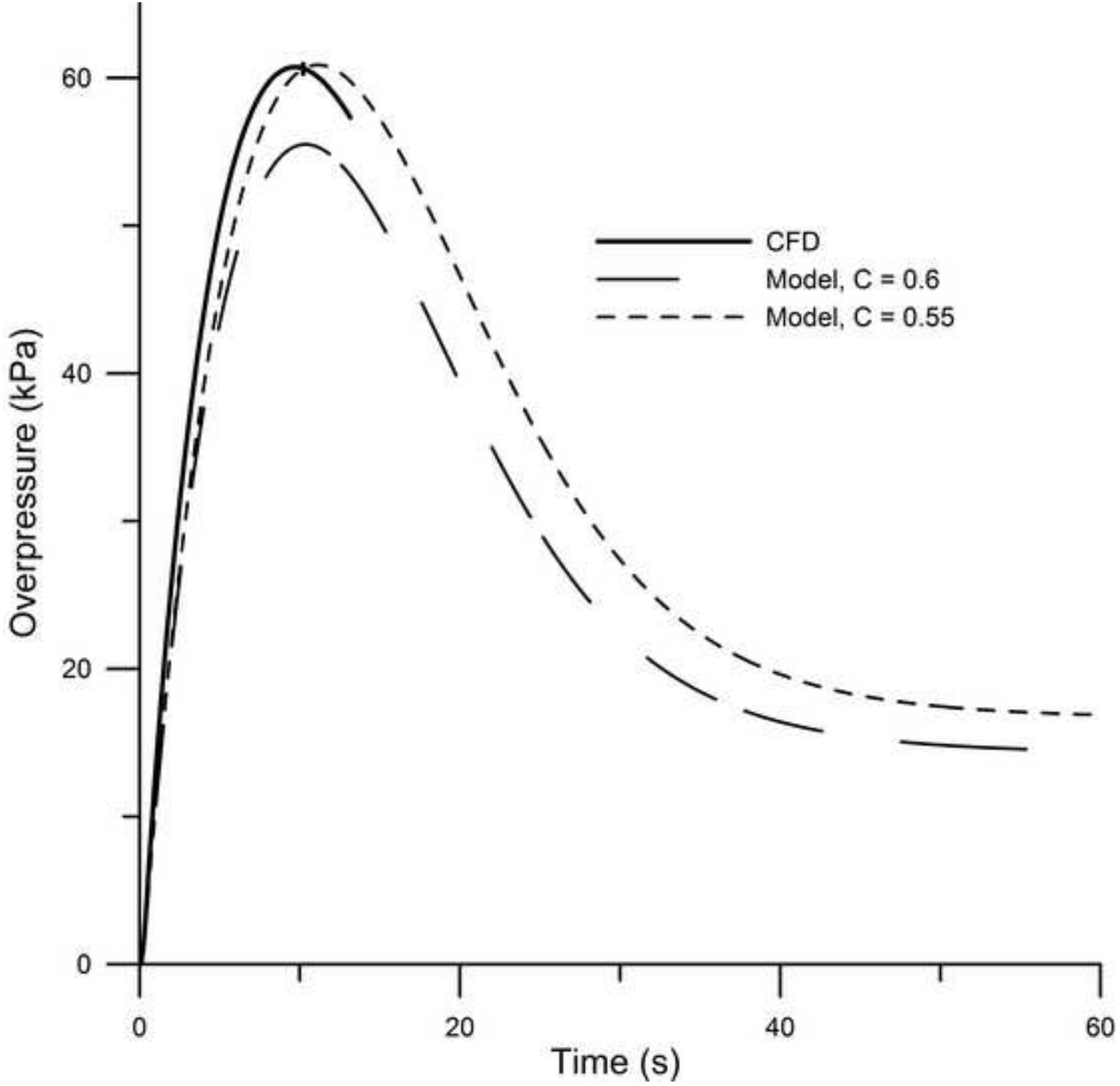

Figure 11

Click here to download high resolution image

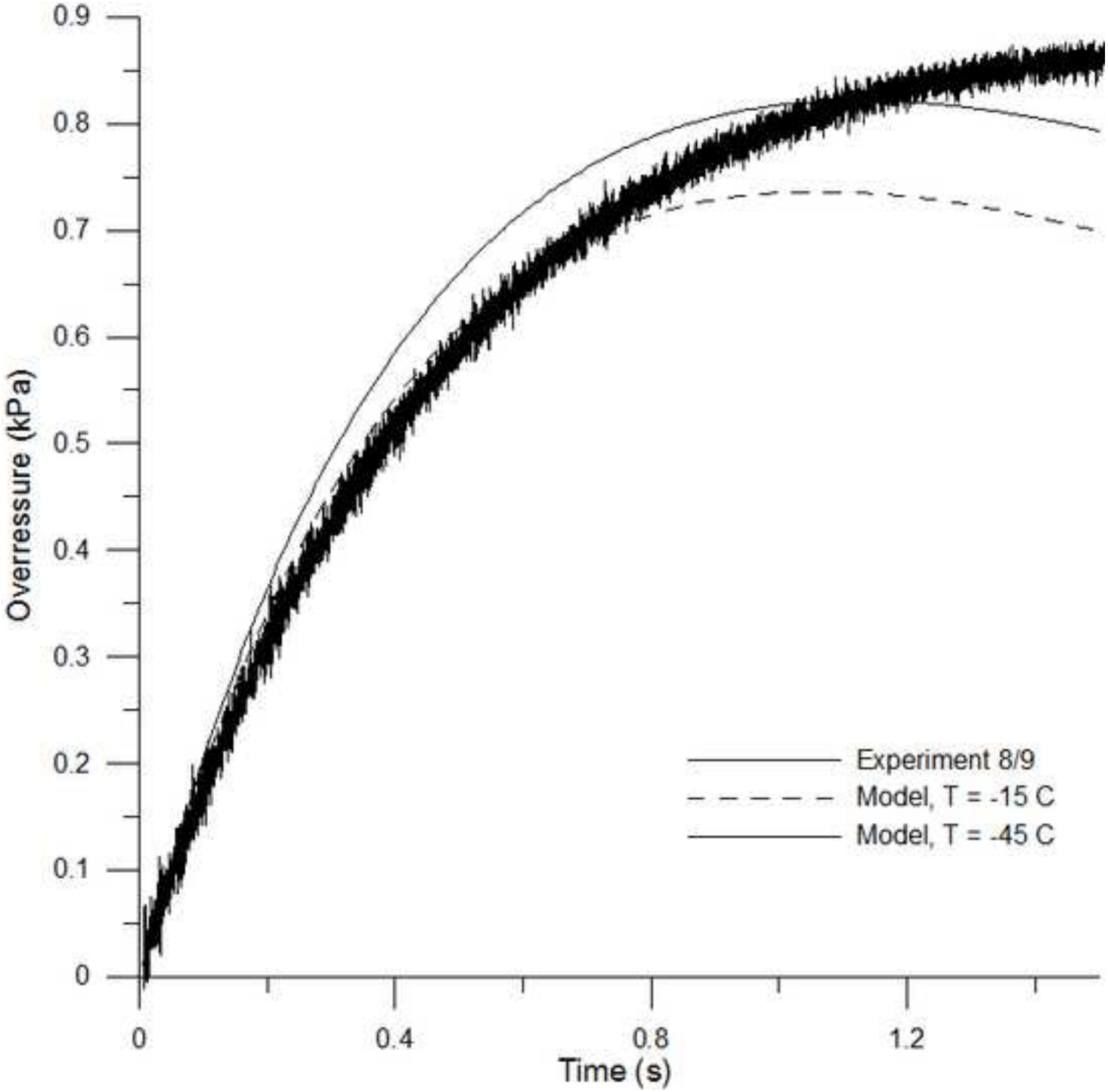

Figure 12

Click here to download high resolution image

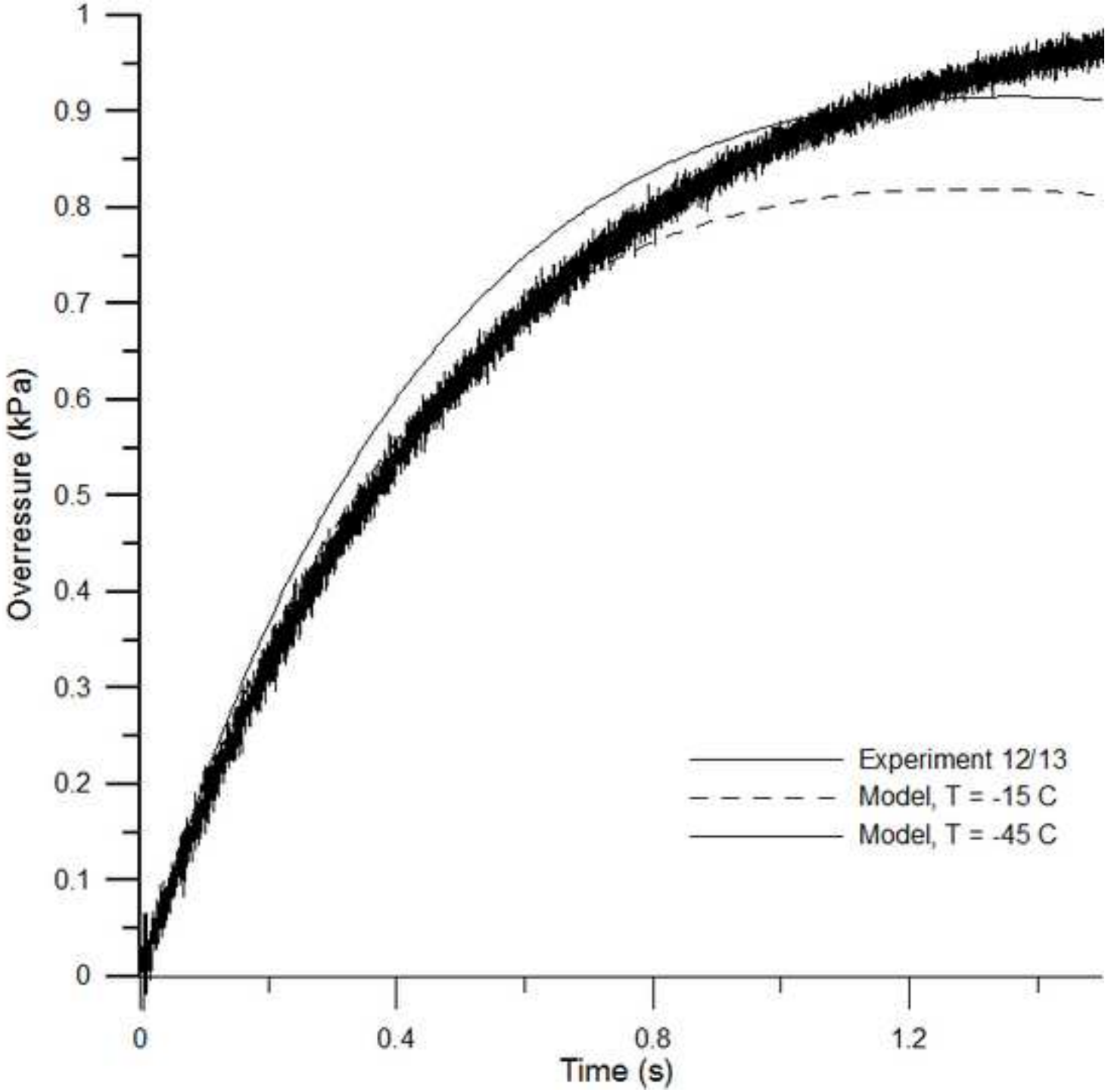

List of figures

Click here to download Supplementary Material: List of figures.docx